

UNCLASSIFIED

Defense Technical Information Center  
Compilation Part Notice

ADP011119

TITLE: Active Control of Forebody Vortices on a schematic Aircraft Model

DISTRIBUTION: Approved for public release, distribution unlimited

This paper is part of the following report:

TITLE: Active Control Technology for Enhanced Performance Operational Capabilities of Military Aircraft, Land Vehicles and Sea Vehicles  
[Technologies des systemes a commandes actives pour l'amelioration des performances operationnelles des aeronefs militaires, des vehicules terrestres et des vehicules maritimes]

To order the complete compilation report, use: ADA395700

The component part is provided here to allow users access to individually authored sections of proceedings, annals, symposia, etc. However, the component should be considered within the context of the overall compilation report and not as a stand-alone technical report.

The following component part numbers comprise the compilation report:

ADP011101 thru ADP011178

UNCLASSIFIED

# Active Control of Forebody Vortices on a Schematic Aircraft Model

R. Lee\* and R. J. Kind†

Carleton University, 1125 Colonel-By-Drive Ottawa  
Ontario, Canada K1S 5B6

E. S. Hanff‡

National Research Council, Ottawa, Ontario, Canada K1A 0R6

A wind-tunnel experiment has been performed to further investigate the potential of the dynamic manipulation of forebody vortices as a means of supplementing directional control of fighter aircraft at high angles of attack. Tests were conducted on a 65-deg delta-wing model fitted with a slender, pointed tangent-ogive forebody of circular cross-section. Forward-blowing nozzles located near the apex of the forebody served as the means of perturbing the forebody vortices. Results have shown that a linear relationship exists between the time-average yawing moment coefficient and a duty cycle parameter. These results, however, are accompanied by a peculiar reversal of yawing moment and side force that occurs when the blowing momentum exceeds a particular threshold value. Cross-coupling effects were also identified between the control method and time-average rolling moment, pitching moment, and normal force.

## Nomenclature

$b$	wing span
$c$	mean geometric chord
$\bar{C}_l$	time-average rolling moment coefficient, ( $1/n \sum_1^n \mathcal{L}$ )/ $q_\infty S b$
$\bar{C}_m$	time-average pitching moment coefficient, ( $1/n \sum_1^n M$ )/ $q_\infty S c$
$\bar{C}_n$	time-average yawing moment coefficient, ( $1/n \sum_1^n N$ )/ $q_\infty S b$
$\bar{C}_Y$	time-average side force coefficient, ( $1/n \sum_1^n Y$ )/ $q_\infty S$
$\bar{C}_Z$	time-average normal force coefficient, ( $1/n \sum_1^n Z$ )/ $q_\infty S$
$C_\mu$	coefficient of blowing momentum, $\dot{m}_j V_j / q_\infty S$ (positive for starboard blowing)
$d$	nozzle diameter
$D$	base diameter of forebody shell
$L$	total length of model
$\dot{m}_j$	nozzle mass flowrate, $\rho \pi d^2 V_j / 4$
$n$	number of sample points within an ensemble-averaged record
$q_\infty$	freestream dynamic pressure, $\rho V_\infty^2 / 2$
$R$	forebody cross-sectional radius at $x$
$Re_D$	Reynolds number, $V_\infty D / \nu$
$S$	wing reference area
$T$	period of an alternating blowing cycle
$V_\infty$	freestream velocity
$V_j$	blowing velocity at nozzle exit
$x_n$	longitudinal location of nozzle exit relative to the nose apex
$\alpha$	angle of attack
$\beta$	angle of sideslip
$\theta$	azimuthal location of nozzle exit relative to the windward meridian

\*Graduate Student, Dept. of Mechanical and Aerospace Engineering.

†Professor, Dept. of Mechanical and Aerospace Engineering.

‡Senior Research Officer, Aerodynamics Laboratory.

$\tau$	duration a valve is open during the alternating blowing cycle
$\omega$	angular frequency of alternating blowing
$\omega^*$	reduced frequency of alternating blowing, $\omega D / V_\infty$

## Introduction

The manipulation of forebody vortices has been recognized as a possible means for augmenting directional control of high-performance aircraft maneuvering in the post-stall flight regime. The approach is attractive for flight control at high angles of attack as it permits the generation of large side forces and yawing moments when the vertical tail(s) has lost its effectiveness.

Several techniques of manipulating the forebody vortices have been investigated.<sup>1,2</sup> Most methods are essentially steady schemes producing quasi-steady loads by forcing the forebody vortices into desired positions with respect to the forebody. To overcome the inherent bi-stability of the forebody vortices that prevails over a significant range of angles of attack, steady methods involve first forcing the vortices to adopt a symmetrical stance, typically by choosing an appropriate forebody geometry. Desired side forces and yawing moments are then generated by coercing the vortices into an asymmetric orientation by either pneumatic or mechanical means. The need to overcome the artificially induced symmetry may require considerable control power. Furthermore, it is difficult to implement suitable control laws due to the severely non-linear response of the vortices, and thus resulting loads, to the control variable.

## Principle of Dynamic Vortex Manipulation

This paper outlines an active, oscillatory, vortex control scheme that has the potential to overcome the

problems associated with steady control methods. The principle is illustrated in Fig. 1. Unlike the steady methods, this scheme takes advantage of the bi-stable nature of the forebody vortices and makes use of the widely known fact that minute disturbances to the flow in the vicinity of the forebody tip can cause the forebody vortices to switch between their two stable states. Specifically, the scheme requires the forebody vortices to be deliberately switched, back and forth, between the two stable states at a sufficiently high frequency that the inertia of the aircraft prevents it from responding to the instantaneous loads. The aircraft would, however, respond to the time-average load which is controlled by varying the fraction ( $\tau/T$ ) of the switching-cycle period during which the vortices are in one state or the other. Load modulation is accomplished with intermittent perturbations of fixed intensity as opposed to variable intensity (of nozzle or slot flow rates, or strake deflection) which is required with steady schemes. Ideally the side force and yawing moment for steady port blowing ( $\tau/T=100\%$ ) would be equal and opposite to that for steady starboard blowing ( $\tau/T=0\%$ ). Then for oscillatory blowing the time-average side force and yawing moment would vary linearly with  $\tau/T$ , being zero at  $\tau/T=50\%$ , as shown in Fig. 1(b).

The deliberate flow perturbation can be implemented by either pneumatic or mechanical means.

### Previous Work

The investigation of this vortex control scheme began with water-tunnel experiments.<sup>3</sup> The model used in these early experiments was an ogive-cylinder with an included apex angle of 60 deg. A hydrodynamic means was used to perturb the vortices. The ogive forebody was fitted with two forward-facing, surface-flush nozzles symmetrically placed near the tip. 'Blowing' fluid could be supplied to either nozzle. By switching the blowing back and forth between the two nozzles it was found that a very low blowing coefficient ( $C_\mu = 0.0013$ ) was sufficient to reliably switch the forebody vortices from one stable configuration to the other at a reasonably high reduced frequency ( $\omega^* = 0.16$ ). Having established that the forebody vortices would respond to oscillatory forward-blowing, the next phase in the investigation was to determine the variation of the time-average side force and yawing moment as a function of blowing duty cycle parameter,  $\tau/T$ . Scaled up tests were performed in a wind tunnel using a version of the water-tunnel model.<sup>4</sup> Forward-blowing nozzles were again used as the perturbation method. Figure 2 shows the key results from these experiments. Note the linear variation of time-average yawing moment and side force coefficients with duty cycle for any particular angle of attack,  $\alpha$ . Only for  $\alpha=70$  deg is there some non-linearity. Note also, however, that the variation with  $\alpha$  is highly non-linear

reflecting the influence of  $\alpha$  on the forebody vortex behaviour for steady or zero blowing (i.e., no vortices, symmetric vortices, asymmetric vortices for low, moderate and high  $\alpha$ , respectively). The sign reversal of  $\bar{C}_n$  in Fig. 2 indicates that the center of pressure moves aft of the moment reference point for  $\alpha=40$  deg.

The present paper focusses on work performed in subsequent wind-tunnel tests using a schematic aircraft model. The main objective of these tests was to ascertain whether the excellent results obtained on the simple ogive-cylinder models could be replicated on a more realistic aircraft-like configuration.

## Experimental Setup

The investigation was conducted in the 2m  $\times$  3m low-speed, closed circuit wind tunnel at the National Research Council of Canada.

### Model

The schematic aircraft model used in these experiments, Fig. 3, features a 65 deg delta-wing, a vertical tail, and a long slender forebody. This model was originally designed for dynamic wind-tunnel experiments at high roll and pitch rates. The forebody of the model has a circular cross-section and a tangent-ogive profile with an apex semi-angle of 12.8 deg. Once again forward blowing was used as the vortex perturbation method. The forebody was designed to accept interchangeable tips so that a series of nozzle locations could be readily tested. Emphasis was placed on locating the nozzle exits closer to the apex than in the previous tests in order to enhance blowing effectiveness. As shown in Fig. 4, the removable tip is 6.35cm long, containing symmetrically-placed nozzles oriented parallel to the forebody axis of revolution. The nozzles have a diameter of 1.52mm ( $d/D=0.0191$ ), which was found to be the smallest possible size that could be drilled without significant deviation of the drill path.

The redesign of the model's forebody also involved the installation of a blowing system within its cavity. The system comprised two miniature solenoid on/off pneumatic valves to control the flow to the nozzles, two flow metering orifices in series with the delivery ports of the valves, and the tubes that delivered the air to the nozzles in the tip. A differential pressure transducer was placed across each metering orifice to measure the flow on the basis of a calibration of the pressure drop as a function of volume flow rate, which was measured with a rotameter-type flow meter. The valves were fed with regulated shop air via a supply tube carried inside the support assembly and hollow balance. The valves were controlled by the data acquisition system.

### Model Support

The model was sting-mounted on a vertical strut attached to turntables located in the floor and ceiling of the test section. The turntables were used to set the body inclination relative to the freestream, see

Fig. 5. The sting and model could be rolled such that combinations of turntable angle and roll angle could produce a range of angles-of-attack and sideslip. An internal five-component balance (no axial force) measured aerodynamic forces and moments in the body axes. A blockage correction was applied to the dynamic pressure using the simple 1/4-area ratio.<sup>5</sup>

#### Data Acquisition

Balance and pressure data (from the nozzle blowing system) were acquired by a computer featuring a real-time UNIX operating system and equipped with a high-performance digital signal processing (DSP) module. The DSP module included a 16-channel A/D converter board with a sampling rate of 150 kHz per channel. Ten channels were used to acquire balance data, pressure data and the solenoid-valve drive waveforms. The data acquisition process was synchronized with the valve drive waveforms and ensemble-averages over many blowing cycles were taken to minimize the effect of noise. The data acquisition system also generated the valve drive waveforms. Time-average results for moments and forces are the arithmetic mean of the respective ensemble-average waveform.

Validation of the complete system was achieved by comparing loads (without blowing) with those acquired for the same model and test conditions in a previous test in a different facility. The results agreed very well.

#### Limitations

A preliminary wind-tunnel entry revealed a serious vibration condition in which the model entered into a diverging lateral oscillation in its yaw plane at the resonance frequency of the model-support system. This was encountered frequently. A pattern in the combination of angle of attack and freestream velocity could not be detected, however, the tendency of the model to vibrate was reduced at lower freestream velocities. The source of excitation was suspected to be a positive feedback between the motion-induced sideslip, which may have switched the vortices, and the resulting change in side force. This appeared to be confirmed by the fact that blowing high-pressure air through one nozzle alleviated the vibration, presumably by preventing further switching of the vortex positions. It is important to note that the vibration problem is an artifact of these experiments as it results from the presence of a rather high frequency resonance due to the model-support stiffness. Such a resonance would be unlikely in free flight because the reduced frequency of normal modes, such as Dutch roll, of the aircraft would be much lower. Nevertheless designers should beware of possible coupling with modes of the flight control system. An emergency system was subsequently put in place that automatically applied the necessary steady blowing once the amplitude of the vibration, as sensed by suitably oriented accelerometers mounted on the

platform of the above mentioned blowing system, exceeded a prescribed threshold. This emergency measure proved to be very successful in suppressing the oscillation in the vast majority of cases. It is interesting to note that the model displayed a lesser tendency to vibrate when the tips with nozzles located closest to the apex, were installed. This suggests that the nozzle cutouts in the vicinity of the apex tended to stabilize the forebody vortices by providing an edge that fixed flow separation. As a consequence of the vibration problem, the majority of the test cases were limited to a freestream velocity of 18.3 or 36.6 m/s. This prevented the study of behaviour at Reynolds number,  $Re_D$ , above  $2.0 \times 10^5$ .

## Results and Discussion

Results are presented in non-dimensional form as coefficients of time-average yawing moment ( $\overline{C}_n$ ), pitching moment ( $\overline{C}_m$ ), rolling moment ( $\overline{C}_\ell$ ), side force ( $\overline{C}_Y$ ) and normal force ( $\overline{C}_Z$ ). The uncertainties in these measurements are estimated to be  $\pm 0.0015$ ,  $\pm 0.0065$ ,  $\pm 0.002$ ,  $\pm 0.035$ , and  $\pm 0.025$  respectively. The sign convention for the moments and forces, and all aerodynamic angles are shown in Fig. 3. Results for Tip 6-1 ( $x_n/D = 0.095$ ,  $\theta = 120$  deg) are presented for a freestream velocity of 36.6 m/s, except in Figs. 8 and 9.

The coefficient of blowing momentum is considered positive when air is applied through the starboard nozzle, and negative through the port nozzle. Nozzle blowing was always asymmetric, that is, blowing was applied to either the starboard or port nozzle, not to both simultaneously. The uncertainty in  $C_\mu$  is about  $\pm 0.0001$ .

#### Typical Result of Dynamic Blowing

Figure 6 shows a typical response of time-average moments and forces to duty cycle for  $\alpha = 45$  deg. The symmetry and linearity in the variation of  $\overline{C}_n$  is considered to be very good. The magnitudes of  $\overline{C}_n$  under steady blowing conditions ( $\tau/T = 0$  and 100%) compare very well with each other; for  $\tau/T = 50\%$ ,  $\overline{C}_n$  is not precisely zero, but at only 3% of the largest value under steady blowing conditions, the result is considered to be reasonable. The results for  $\overline{C}_n$  conform to expectations (Fig. 1) and to the previous results with the ogive-cylinder model (Fig. 2). The variation of  $\overline{C}_Y$  is somewhat non-linear but note the low values, and thus degraded measurement accuracy, compared with the normal force,  $\overline{C}_Z$ . The principal difference from the previous results (Fig. 2) is the reversed slope of the linear variation. The cause of this will be discussed later.

Preliminary measurements were performed in order to obtain an estimate of the response time of the forebody vortices to the deliberate perturbations. Unfortunately results were insufficiently reliable to enable

an estimate to be made.

A cross-coupling effect between forebody vortex control and rolling moment is revealed by the linear variation of  $\bar{C}_\ell$  with duty cycle, Fig. 6(e). This effect is thought to arise from the potential of a forebody vortex to strongly influence a wing leading-edge vortex.<sup>6,7</sup> The linearity of  $\bar{C}_\ell$  is distorted somewhat at duty cycle values below 20% and above 80%. An examination of the instantaneous data indicates that the local non-linearity is due to a 'cutoff' of the instantaneous rolling moment as the vortices are switched, i.e., there is not enough time for the rolling moment to reach the magnitude arising from the other vortex orientation, before being forced to change back again. This non-linearity would disappear at lower reduced frequencies. Although  $\bar{C}_\ell$  is not precisely zero at 50% duty cycle, it is much less than for no-blowing conditions (natural vortex asymmetry). This result confirms an earlier finding<sup>5</sup> that alternating blowing using a 50% duty cycle has the potential to eliminate asymmetric rolling moments due to forebody vortex asymmetry. Note that the rolling moment is positive when yawing moment is positive, and vice versa, a favourable juxtaposition for maneuvering.

The variation of  $\tau/T$  was found to have a small effect on  $\bar{C}_m$  and  $\bar{C}_Z$ . For  $\alpha=45$  deg, as in Fig. 6(c) and (d), the nominal zero-blowing values of  $\bar{C}_m$  and  $\bar{C}_Z$  are 0.011 and 1.464 respectively, only a little lower than some values seen in Fig. 6 for dynamic blowing. The small magnitude of  $\bar{C}_m$  indicates that the center of pressure for  $\bar{C}_Z$  is close to the moment reference center. Furthermore, the variation in  $\bar{C}_m$  is slight, signifying that the center of pressure has a very small range of movement. The small travel and close proximity of the center of pressure to the reference center are strong indicators that the increase in  $\bar{C}_Z$ , with dynamic blowing, is the result of an increased contribution by the wing rather than the forebody. As will be seen later, the switching of the forebody vortices causes a definitive increase in the normal force at lower angles of attack.

#### Effect of $C_\mu$

The effect of  $C_\mu$  on the time-average static yawing moment and side force is depicted in Fig. 7. The response of  $\bar{C}_n$  and  $\bar{C}_Y$  to  $C_\mu$  are comparable although the side force results are thought to be affected by additional side forces unrelated to blowing, acting near the moment reference center. Examining the yawing moment response, it is seen that as negative (port) blowing momentum increases from zero,  $\bar{C}_n$  remains reasonably constant at the baseline magnitude. Positive  $\bar{C}_n$  signifies that the port vortex is situated farther above the forebody than the starboard vortex. However at  $C_\mu \simeq -0.0013$ ,  $\bar{C}_n$  begins to decrease rapidly until at  $C_\mu \simeq -0.0025$ ,  $\bar{C}_n$  has changed sign and stabilized at -0.075, nearly the same magnitude as before

the change in sign. Clearly the arrangement of the vortices has switched from one stable state to the other. The 'reversal' of sign is also observed for positive  $C_\mu$ , i.e.,  $\bar{C}_n$  changes from negative to positive at approximately the same magnitude of  $C_\mu$ . It is noteworthy that very little blowing ( $C_\mu \simeq 0.0004$ ) is required to switch the vortices away from their zero-blowing arrangement which happens to be that which gives positive  $\bar{C}_n$  for the present model. Generally the magnitude of  $\bar{C}_n$  is approximately the same before and after the reversal for either starboard or port blowing. Surface flow visualization conducted in the wind tunnel, supported by off-surface flow visualization using the forebody only in a water tunnel, verified the switching of the vortex arrangement as the magnitude of  $C_\mu$  surpassed a threshold value. Also, in the water tunnel, it was observed that the reversal coincided with the blowing jet penetrating through the shear layer into the freestream flow. All dynamic blowing results presented in this paper are associated with a value of  $C_\mu$  beyond the reversal threshold.

This reversal phenomenon could be undesirable from a flight control perspective. It is not perceived to be a serious problem with the present control scheme, however, as a  $C_\mu$  magnitude significantly above the threshold, or below, could be used for dynamic blowing.

#### Effect of Angle of Attack

As seen in Fig. 8 the variation of  $\bar{C}_n$  and  $\bar{C}_\ell$  with duty cycle is reasonably linear as the angle-of-attack is changed. It is evident in Fig. 8 that for  $\alpha$  below the onset value for forebody vortex asymmetry  $\bar{C}_n$  is very small and essentially independent of the blowing duty cycle. This is obviously not a problem as at such low angles-of-attack the rudder has sufficient control authority. As  $\alpha$  increases and vortex asymmetry develops, the slope of the linear variation of  $\bar{C}_n$  also increases. For  $\alpha > 45$  deg the slope decreases from its maximum, reflecting the variation of  $\bar{C}_n$  with  $\alpha$  for steady blowing. The behaviour of  $\bar{C}_\ell$  is similar. The slope of  $\bar{C}_\ell$  versus  $\tau/T$  becomes nearly zero by  $\alpha = 55$  deg. Time-average side force is very small and trends in the data are thus ambiguous due to poor signal-to-noise ratio. For  $C_\mu$  within the reversal range, the results for  $\bar{C}_n$  show less linearity and less symmetry between steady port and starboard blowing conditions.

The results for time-average normal force show an interesting gain in  $\bar{C}_Z$  at some  $\alpha$  values for alternating blowing as opposed to steady blowing. This is particularly evident for  $\alpha = 35$  deg and  $\tau/T = 50\%$ , where the increase is about 15%. At that condition  $\bar{C}_n$  and  $\bar{C}_\ell$  are small or zero indicating that the increase in  $\bar{C}_Z$  is not accompanied by ancillary effects in the other axes. It appears that this effect results from the influence of the forebody vortices on the leading-edge

vortex breakdown locations, which largely depends on the relative position of the corresponding vortices on each side. Under alternating blowing conditions, the varying interaction between the forebody and leading-edge vortices leads to a corresponding modulation of the latter's breakdown locations. It is known however, that the aft propagation speed of breakdown is considerably higher than its forward propagation speed,<sup>8</sup> thus, under dynamic conditions, the average location of breakdown is further aft than the corresponding static value, leading to the observed increase in normal force.

### Effect of Reduced Frequency

The frequency of alternating blowing is an important parameter in the dynamic manipulation of forebody vortices. Forcing the vortices to switch at the highest frequency practicable will reduce the amplitude of oscillation of the aircraft. Conceivably, a reduced amplitude should ease pilot fatigue – a serious concern in view of the vibratory nature of the technique – and improve the pilot's ability to target weapons. Conversely, operation at a higher frequency would exacerbate possible structural fatiguing of the forebody.

Figure 9 presents results for three reduced frequencies ranging from  $\omega^* = 0.16$  to 0.48. For  $V_\infty = 18.3$  m/s, this change in  $\omega^*$  translates into a frequency increase from 5.8 to 17.5 Hz. The linearity of the variation of  $\bar{C}_n$  with duty cycle has remained intact with the increase of  $\omega^*$ . This indicates that the vortices have no difficulty switching back and forth even at the highest  $\omega^*$ , implying that the vortex response time is much less than the period,  $T$ , of the alternating blowing cycle, even at  $\omega^* = 0.48$ . Time-average pitching moment, normal force, and rolling moment all exhibit some response to changes in the reduced frequency. This is thought to be due to the phenomenon discussed in the preceding section. The behaviour is evidently rather complex as the trends seen in Fig. 9 are not monotonic with increasing  $\omega^*$ . The time-average side force coefficient,  $\bar{C}_y$ , remains small at all values of  $\omega^*$ .

### Effect of Sideslip

The effect of sideslip on the variation of time-average forces and moments with duty cycle is shown in Fig. 10 for  $\alpha = 45$  deg.

It is apparent that nozzle blowing continues to be effective with non-zero sideslip. The results presented are for a tip configuration that has the nozzle exits, or cutouts, as close to the apex as practicable ( $x_n/D = 0.095$ ,  $\theta = 120$  deg). In fact the nozzle exit is even closer to the apex than for the tip shown in Fig. 4. It is thought that the large ratio of nozzle diameter to local cross-sectional radius of the forebody is primarily responsible for the continued effectiveness with sideslip. With a large ratio, the fraction of forebody surface area removed by the nozzle cutout is signifi-

cant, allowing the nozzle flow to continuously influence the local shear layer separation process, in spite of the circumferential movement of the primary separation line caused by sideslipping.

The variation of  $\bar{C}_n$  remains linear with duty cycle under sideslipping conditions. In Fig. 10(a)  $\partial\bar{C}_n/\partial\beta$  is negative, indicating directional instability, as would be expected at high angles of attack due to blanketing of the vertical tail. Figure 10(c) reveals a cross-coupling effect between pitching moment,  $\bar{C}_m$ , and duty cycle,  $\tau/T$ . Specifically, sideslip gives rise to a linear variation of  $\bar{C}_m$  with duty cycle. For a given sideslip angle, a duty-cycle sweep is sufficient to change the sign or sense of  $\bar{C}_m$ . Since  $\bar{C}_Z$  is always positive this implies movement of the centre of pressure. Shifting of the centre of pressure for  $\bar{C}_Z$  is probably due to a more intense influence, or lack thereof, of the forebody vortices on the upper-surface (body axis) static pressure of the forebody. For example, with a positive sideslip angle of  $\beta \approx 15$  deg and starboard blowing stronger than the reversal threshold (i.e.,  $C_\mu > 0.0025$  and  $\tau/T = 0\%$ ), the starboard forebody vortex is attached and crosses over close to the upper surface of the forebody thus causing a positive increment in  $\bar{C}_m$  relative to the zero-sideslip,  $\tau/T = 50\%$  datum case. On the other hand, with port blowing,  $\tau/T = 100\%$ , the starboard vortex will be detached and will pass relatively far above the forebody, having little effect on the static pressure on the upper surface of the forebody. The static pressure will consequently be higher than the datum case, giving rise to a negative increment in  $\bar{C}_m$ . The conjectured behaviour illustrated by this example is precisely what is seen in Fig. 10(c). In both of these duty-cycle cases the port forebody vortex will pass relatively far from the port side of the forebody, due to the sideslip velocity component, and will thus have little influence on the forebody pressure distribution.

The rolling-moment versus  $\tau/T$  curves in Fig. 10(e) are approximately parallel to one another for all values of the sideslip angle. This indicates that sideslip affects rolling moment mainly by virtue of the conventional mechanism for delta-wings, namely higher effective incidence on the upwind wing panel and lower on the leeward panel.

## Concluding Remarks

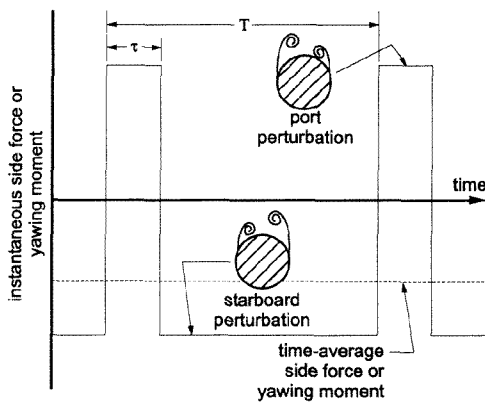
A scheme for actively controlling forebody vortices to obtain linear variation of yawing moment at post-stall angles of attack has been briefly reviewed. The concept involves oscillatory perturbation of the flow-field near the forebody apex and it has the potential to overcome the problems associated with steady vortex control methods. The results of wind tunnel tests using a schematic aircraft model are presented. Using forward blowing as the means of perturbing the vortices, these tests have shown that the proposed method of control is feasible on realistic aircraft configura-

tions. Significant differences, however, exist between the current results and those obtained with an earlier ogive-cylinder model. In the most recent experiments, the signs of the time-average yawing moment and side force were found to change when the nozzle blowing momentum exceeded a certain threshold value. Linearity of  $\bar{C}_n$  with duty cycle is still observed.

With an aircraft configuration, cross-coupling effects on the roll and pitch axes are to be expected and were indeed observed. A range of angle of attack, sideslip angle and reduced frequency was investigated. An intriguing result was a gain in time-average normal force that occurs with 50% duty cycle and zero sideslip. Qualitative explanations of this and other results are offered in terms of the direct effects of the forebody vortices and the significant influence that forebody vortices can exert on delta-wing leading-edge vortices.

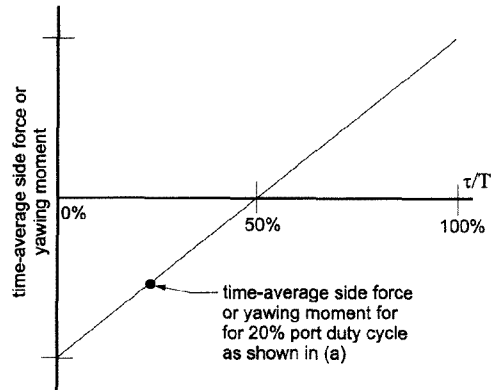
**References**

- <sup>1</sup>Malcolm, G., "Forebody Vortex Control - A Progress Review," AIAA Paper 93-3540-CP, August 1993, pp. 1082-1116.
- <sup>2</sup>Williams, D., "A Review of Forebody Vortex Control Scenarios," AIAA Paper 97-1967, June 1997.
- <sup>3</sup>Alexan, K., Hanff, E., and Kind, R., "Water-Tunnel Investigation of Dynamic Manipulation of Forebody Vortices," AIAA Paper 94-0503, January 1994.
- <sup>4</sup>Lee, R., Hanff, E., and Kind, R., "Wind-Tunnel Investigation of Dynamic Manipulation of Forebody Vortices," AIAA Paper 95-1794, June 1995.
- <sup>5</sup>Pope, A. and Rae, W., *Low-Speed Wind Tunnel Testing*, Wiley, New York, 2nd ed., 1984.
- <sup>6</sup>Ng, T., Suarez, C., Kramer, B., Ong, L., Ayers, B., and Malcolm, G., "Forebody Vortex Control for Wing Rock Suppression," *Journal of Aircraft*, Vol. 31, No. 2, March-April 1994, pp. 298-305.
- <sup>7</sup>Crowther, W., Hodgkin, F., and Wood, N., "Forebody Flow Control for Extended High Angle of Attack Manoeuvres," Royal Aeronautical Society Conference, High Lift and Separation Control, Paper 18, March 1995.
- <sup>8</sup>Hanff, E. and Huang, X., "Roll-Induced Cross-Loads on a Delta Wing at High Incidence," AIAA Paper 91-3223, September 1991.



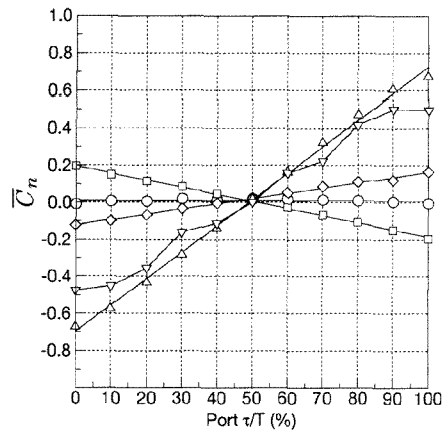
a) Idealized side force or yawing moment time-history.

Fig. 1 Principle of using dynamic manipulation of forebody vortices to control side force and yawing moment.

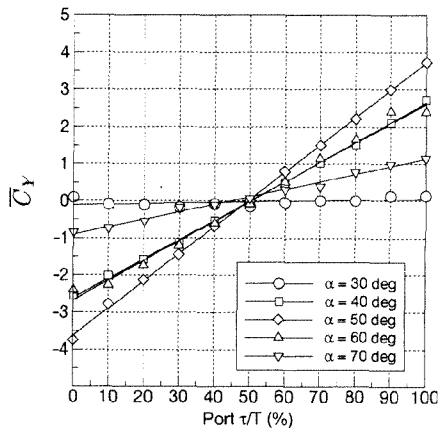


b) Expected variation of time-average side force or yawing moment with duty cycle.

Fig. 1 (continued)



a) Yawing moment



b) Side force

Fig. 2 Variation of  $\bar{C}_n$  and  $\bar{C}_Y$  with duty cycle for an ogive-cylinder model.  $C_{\mu} = 0.00066$ ,  $Re_D = 1.76 \times 10^5$  (19.2 m/s),  $\omega^* = 0.32$  (7.2 Hz),  $\beta = 0$  deg. The moment reference center is  $3.5D$  aft of the forebody apex. (Ref. 4)

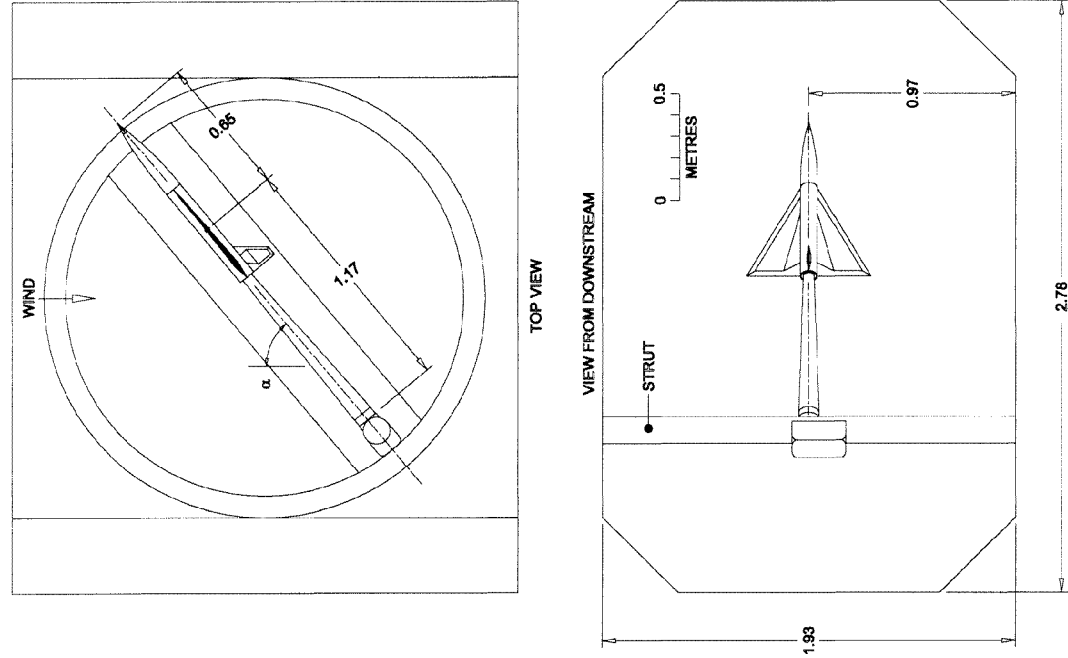


Fig. 5 Two views of the model installation in the working section of the 2m x 3m wind tunnel.

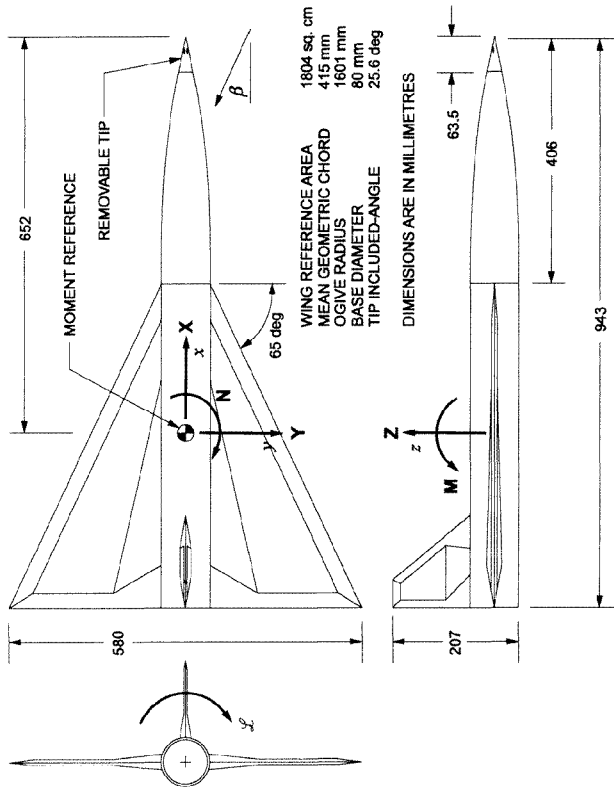


Fig. 3 65-deg delta-wing model with a long, slender forebody of circular cross-section, featuring a removable tip. Forces, moments, and angles are positive as shown.

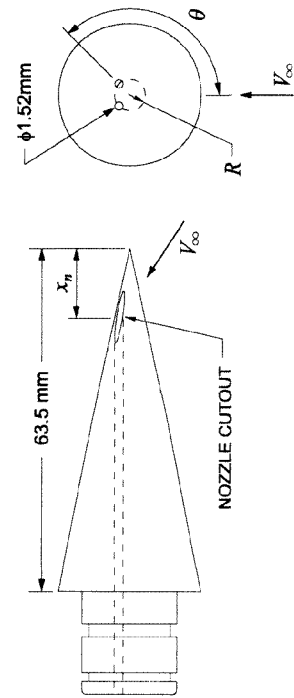
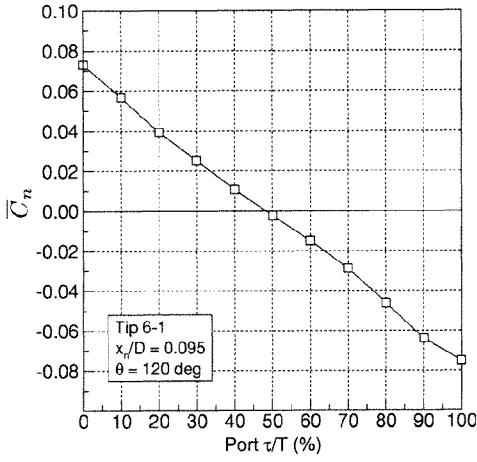
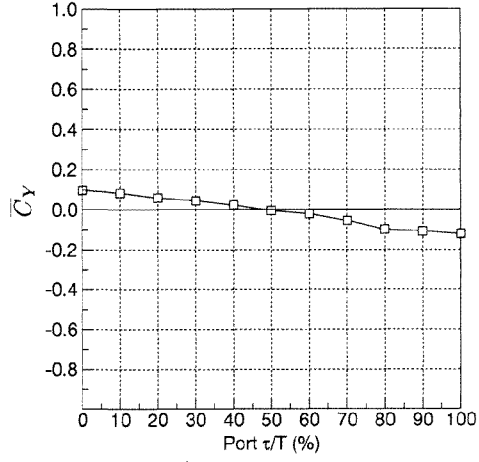


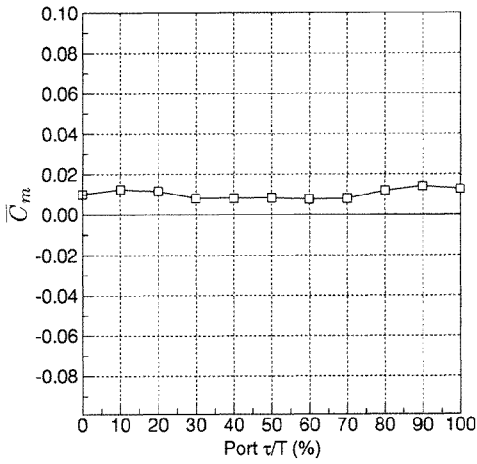
Fig. 4 Schematic of removable forebody tip.



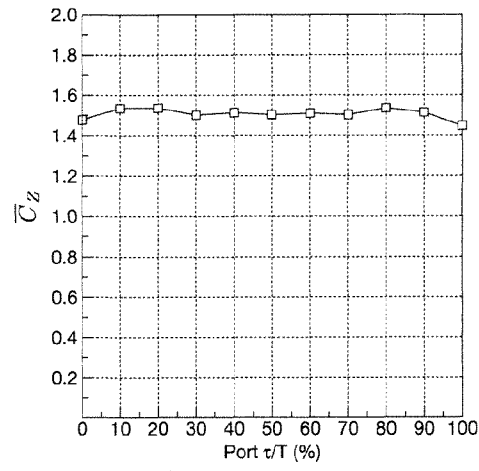
a) Yawing moment



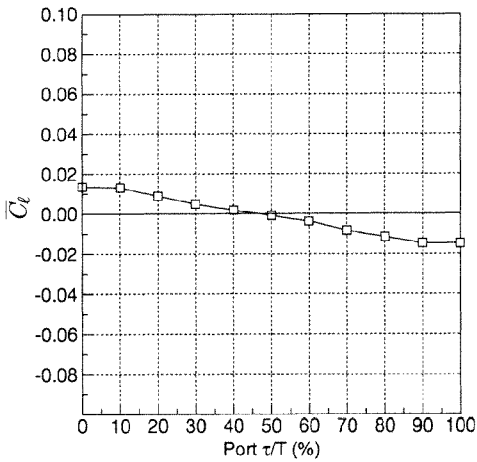
b) Side force



c) Pitching moment

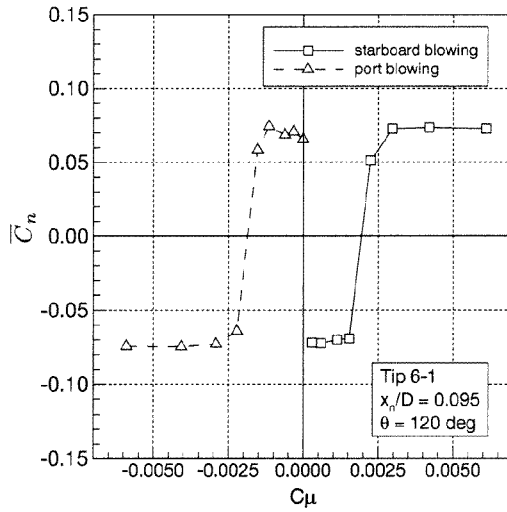


d) Normal force

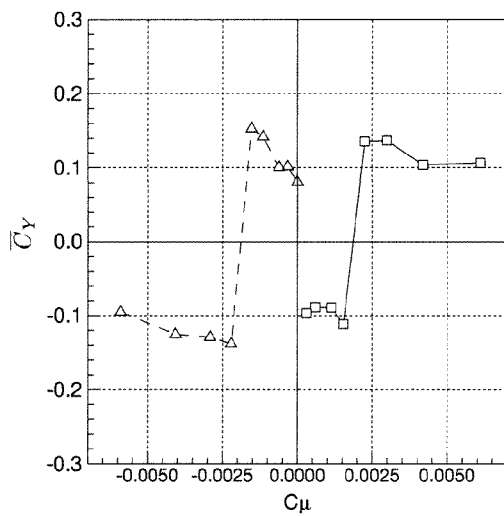


e) Rolling moment

**Fig. 6** Typical variation of time-average forces and moments with duty cycle for the delta-wing model.  $C_\mu = 0.00351$ ,  $Re_D = 2.0 \times 10^5$  (36.6 m/s),  $\alpha = 45$  deg,  $\omega^* = 0.16$  (11.6 Hz), and  $\beta = 0$  deg.

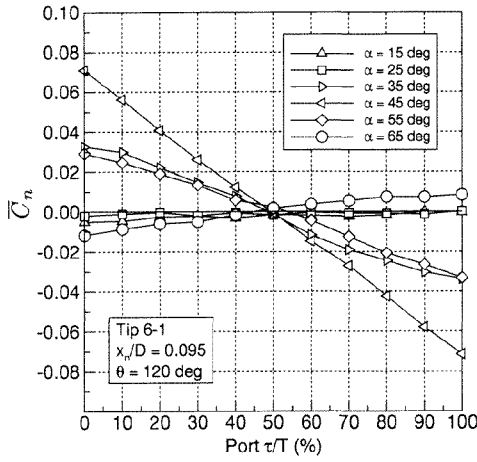


a) Yawing moment

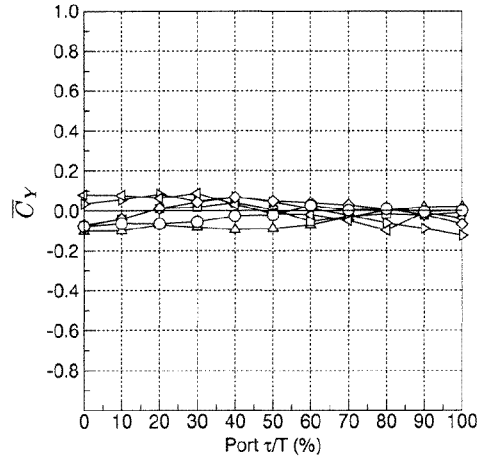


b) Side force

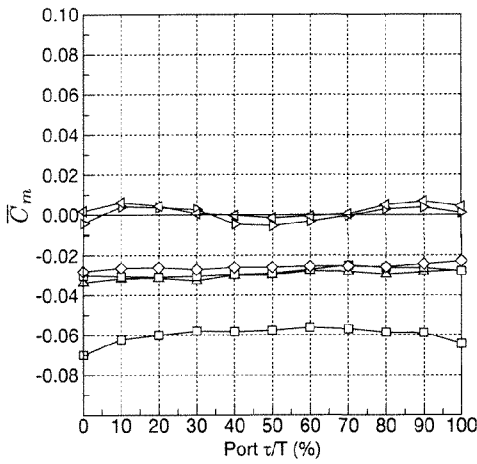
Fig. 7 Variation of time-average yawing moment and side force with blowing moment coefficient for the delta-wing model.  $Re_D = 2.0 \times 10^5$  (36.6 m/s),  $\alpha = 45$  deg, and  $\beta = 0$  deg.



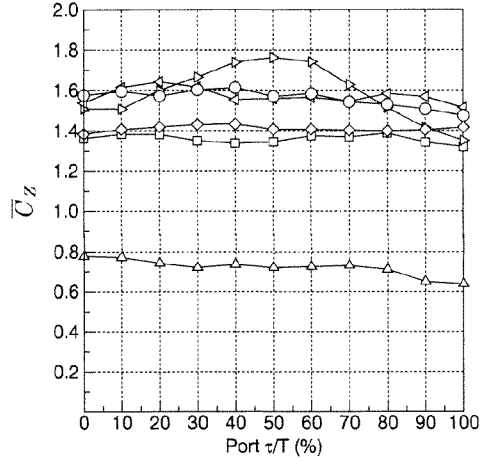
a) Yawing moment



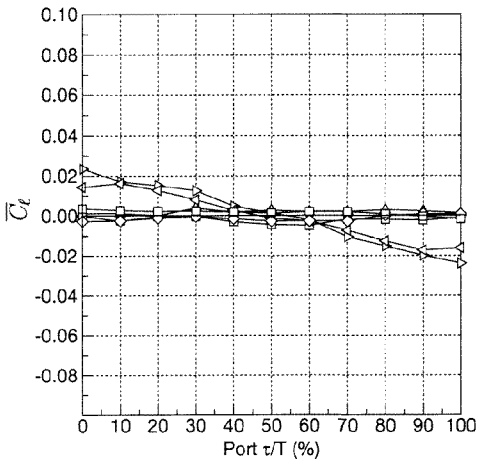
b) Side force



c) Pitching moment



d) Normal force



e) Rolling moment

**Fig. 8** Effect of angle of attack on the variation of time-average forces and moments with duty cycle for the delta-wing model.  $C_{\mu} = 0.00686$ ,  $Re_D = 9.8 \times 10^4$  (18.3 m/s),  $\omega^* = 0.16$  (5.8 Hz), and  $\beta = 0$  deg.

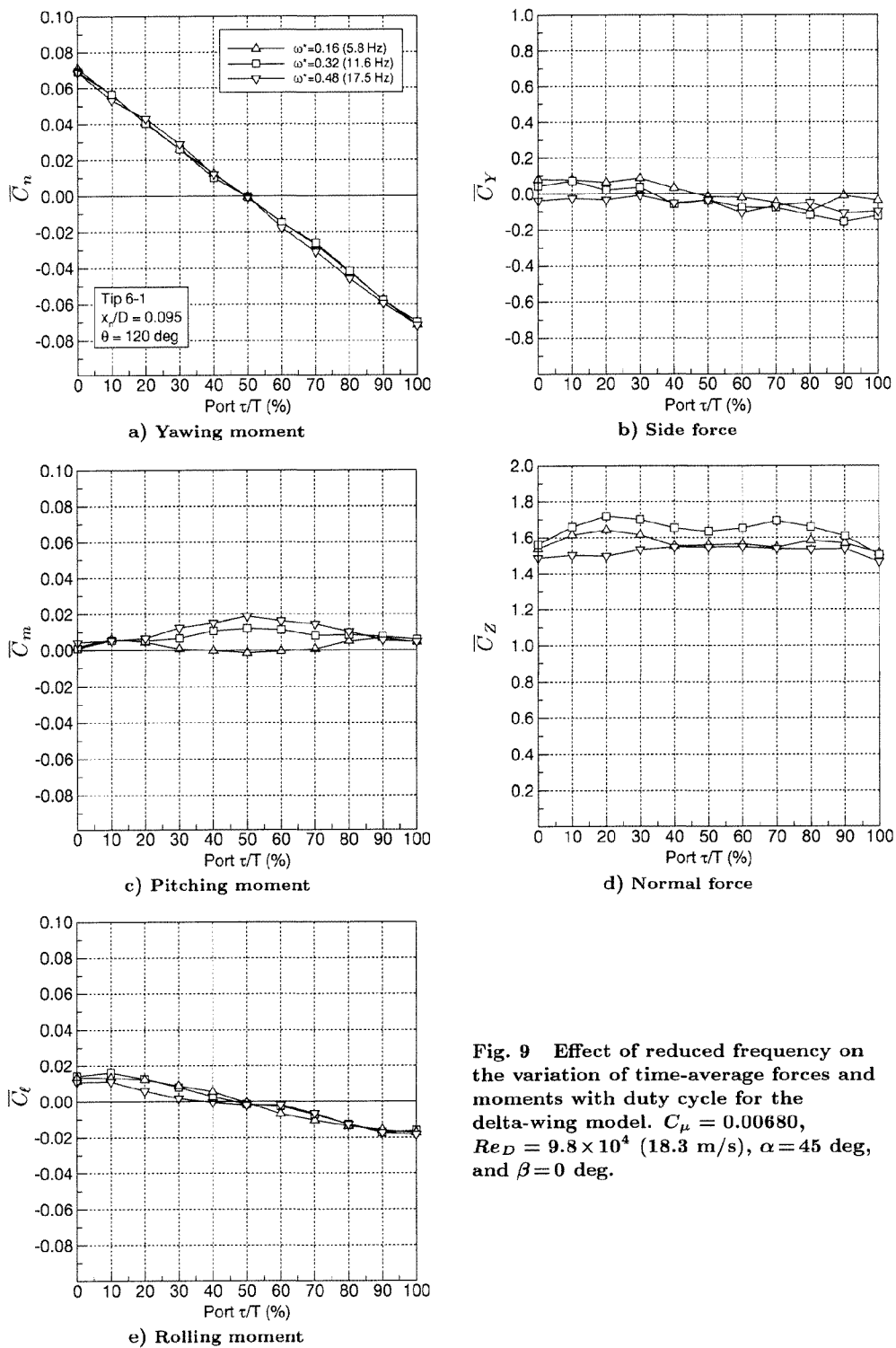
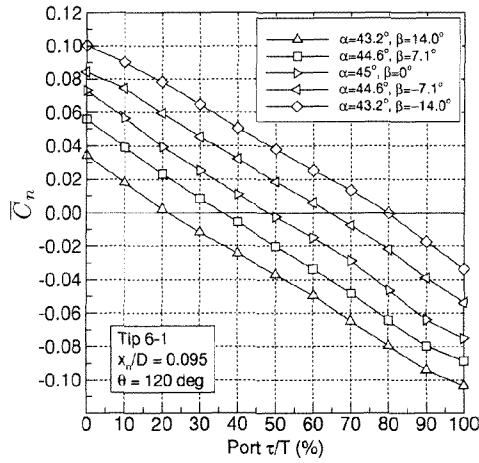
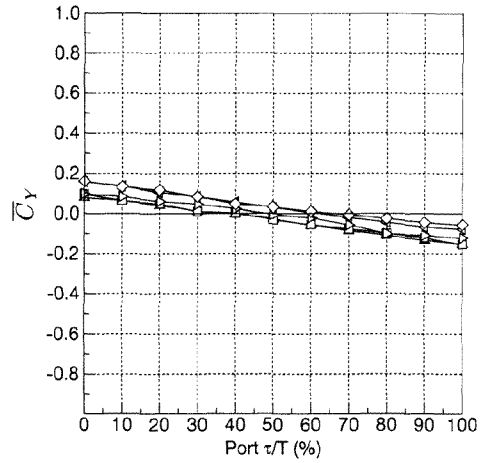


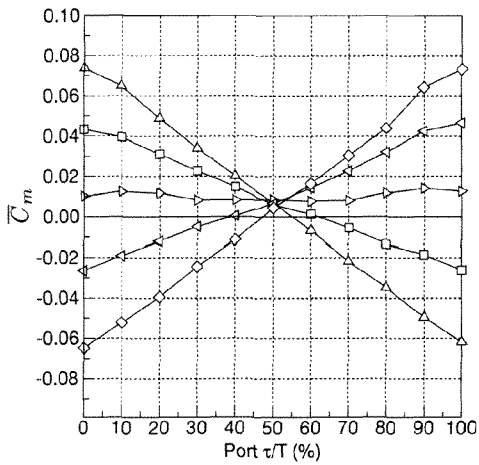
**Fig. 9** Effect of reduced frequency on the variation of time-average forces and moments with duty cycle for the delta-wing model.  $C_\mu = 0.00680$ ,  $Re_D = 9.8 \times 10^4$  (18.3 m/s),  $\alpha = 45$  deg, and  $\beta = 0$  deg.



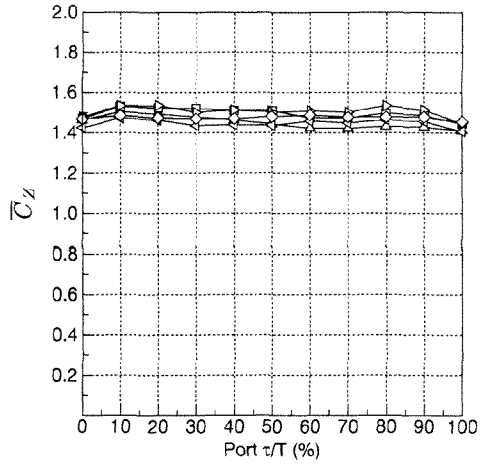
a) Yawing moment



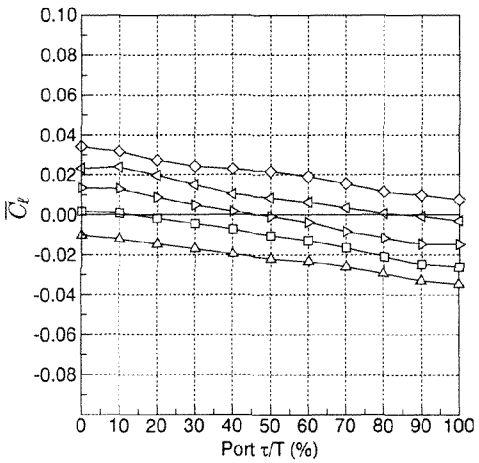
b) Side force



c) Pitching moment



d) Normal force



e) Rolling moment

Fig. 10 Effect of sideslip on the variation of time-average forces and moments with duty cycle for the delta-wing model.  $C_\mu = 0.00351$ ,  $Re_D = 2.0 \times 10^5$  (36.6 m/s),  $\alpha \approx 45$  deg, and  $\omega^* = 0.16$  (11.6 Hz).

Paper #22

Q, by David Moorhouse: Your results showed a linear relationship with blowing, but sensitivity and even reversal with angle of attack. This would be a problem using the results in a full-scale application, would you like to comment.

A (R. Kind): We believe that there is still much wind tunnel testing required before full scale testing would be appropriate. In particular, we need to develop a better understanding of the 'reversal' phenomenon and of the conditions under which it occurs and possibly how to avoid it or best deal with it. Also behaviour of the scheme needs to be explored at much higher Reynolds numbers than the maximum values reached to date. In addition, tests should be done at higher reduced frequencies because we have not yet reached the maximum reduced frequency at which the scheme still works.

Q, by F.R. Grosche: Can you tell us why you chose forward blowing to influence the vortex system?

A (R. Kind): This was an intuitive choice. I had worked on circulation control early in my career; consequently I appreciated that very modest amounts of blowing could be used to influence flow separation and thus cause quite dramatic changes in flow fields and the associated forces and moments. Also we felt that blowing would be easier to implement in practice than suction.

**This page has been deliberately left blank**



**Page intentionnellement blanche**